Theoretical Chemistry Accounts (2018) 137:168
https://doi.org/10.1007/s00214-018-2370-5

REGULAR ARTICLE

Range-separated density-functional theory applied to the beryllium dimer and trimer

Peter Reinhardt[1] · **Julien Toulouse**[1] · **Andreas Savin**[1]

Received: 15 June 2018 / Accepted: 25 September 2018 / Published online: 7 November 2018

Abstract
The beryllium dimer and trimer are, despite their small number of electrons, excellent systems for assessing electronic-structure computational methods. With reference data provided by multi-reference averaged coupled-pair functional calculations, we assess several variants of range-separated density-functional theory, combining long-range second-order perturbation theory or coupled-cluster theory with a short-range density functional. The results show that (i) long-range second-order perturbation theory is not sufficient, (ii) long-range coupled-cluster theory gives reasonably accurate potential energy curves, but (iii) provided a relatively large value of $\mu = 1\,\text{bohr}^{-1}$ for the range-separation parameter is used.

Keywords Density-functional theory · Range separation · Beryllium clusters

1 Introduction

Density-functional theory (DFT) has become in the last 20 years a widely used tool in quantum chemistry due to its good performance for structural and thermochemical properties at an advantageous cost even for medium-size molecules and larger entities. Nevertheless, research is still very active to improve the usual DFT approximations, notably for the treatment of long-range dispersion interactions and the treatment of genuine multi-reference cases.

To address the former issue, János Ángyán, to the memory of whom this article is dedicated, worked on the development of range-separated density-functional theory (RS-DFT), in a long-standing and fruitful collaboration with the present authors (see, e.g., Refs. [1–5]). A never-published work that was started with János some years ago was on the application of RS-DFT on the dimer and trimer of Beryllium, which contain both dispersion and multi-reference effects. For this special issue, we have reexamined this work and completed it.

Be_2 is weakly bound and has been the subject to a long-standing discussion between theoreticians and experimentalists [6–13], whereas Be_3 is a fairly stable aggregate, thus of completely different nature in bonding. This has been reviewed by, e.g., Kalemos in a recent publication [14]. The goal of the present paper is to see whether different flavors of RS-DFT can correctly describe these different chemical bonds.

The paper is organized as follows. After a short recall of RS-DFT, we give a brief survey of existing data and construct consistent reference results for both the dimer and the trimer. To these we compare different flavors of RS-DFT and discuss their performance. All further technical details are collected in "Appendix", and the underlying datasets can be consulted in the Supplementary Material.

2 Range-separated density-functional theory

The common Kohn–Sham procedure [15] minimizes the following energy expression with a single Slater determinant wave function Φ

$$E_{\text{exact}} = \min_{\Phi} \left\{ \langle \Phi | \hat{T} + \hat{V}_{\text{ne}} | \Phi \rangle + E_{\text{Hxc}}\left[n_{\Phi}\right] \right\}, \tag{1}$$

Published as part of the special collection of articles In Memoriam of János Ángyán.

Electronic supplementary material The online version of this article (https://doi.org/10.1007/s00214-018-2370-5) contains supplementary material, which is available to authorized users.

✉ Peter Reinhardt
Peter.Reinhardt@sorbonne-universite.fr

[1] Laboratoire de Chimie Théorique, Sorbonne Université and CNRS, 4 place Jussieu, 75252 Paris, France

where $\hat{T}$ is the kinetic energy operator, $\hat{V}_{ne}$ is the electron–nucleus attraction operator, and $E_{Hxc}[n_\Phi]$ is the Hartree-exchange-correlation functional evaluated at the density n_Φ produced by Φ. With the exact density functional $E_{Hxc}[n]$, the exact ground-state energy would be obtained, in the limit of a complete basis set, by virtue of the Hohenberg–Kohn theorem.

The Kohn–Sham method can be considered as a special case of a more general RS-DFT scheme (see, e.g., Ref. [16])

$$E_{\text{exact}} = \min_{\Psi} \left\{ \langle \Psi | \hat{T} + \hat{V}_{ne} + \hat{W}_{ee}^{lr} | \Psi \rangle + E_{Hxc}^{sr}[n_\Psi] \right\}, \tag{2}$$

where Ψ is a general, multi-determinant wave function, $\hat{W}_{ee}^{lr} = \sum_{i<j} w_{ee}^{lr}(r_{ij})$ is a long-range electron–electron interaction, and $E_{Hxc}^{sr}[n]$ the associated short-range complement Hartree-exchange-correlation density functional. The range separation of the electron–electron interaction

$$\frac{1}{r_{ij}} = w_{ee}^{lr}(r_{ij}) + \left(\frac{1}{r_{ij}} - w_{ee}^{lr}(r_{ij}) \right), \tag{3}$$

is achieved through the use of the error function with an arbitrary parameter μ

$$w_{ee}^{lr}(r_{ij}) = \frac{\text{erf}(\mu\, r_{ij})}{r_{ij}}. \tag{4}$$

In practice, approximations must be used for the wave function Ψ. A first step is to use only a single-determinant wave function Φ, which leads to the range-separated hybrid (RSH) approximation [1]

$$E_{\text{RSH}} = \min_{\Phi} \left\{ \langle \Phi | \hat{T} + \hat{V}_{ne} + \hat{W}_{ee}^{lr} | \Phi \rangle + E_{Hxc}^{sr}[n_\Phi] \right\}, \tag{5}$$

the expectation value of the long-range interaction, $\langle \Phi | \hat{W}_{ee}^{lr} | \Phi \rangle$, giving a long-range Hartree-Fock (HF) contribution to the energy. The minimization in Eq. (5) leads to self-consistent Kohn–Sham-like RSH equations for the orbitals $|\phi_i\rangle$ and orbital energies ϵ_i

$$\left(\hat{T} + \hat{V}_{ne} + \hat{V}_H + \hat{V}_{x,HF}^{lr} + \hat{V}_{xc}^{sr} \right) |\phi_i\rangle = \epsilon_i |\phi_i\rangle, \tag{6}$$

where $\hat{V}_H$ is the full-range Hartree potential, $\hat{V}_{x,HF}^{lr}$ is the long-range nonlocal HF exchange potential (evaluated with the "erf" part of the electron–electron interaction), and $\hat{V}_{xc}^{sr}$ is the short-range exchange-correlation potential (obtained from the functional derivative of $E_{xc}^{sr}[n]$).

Equation (5) does not yet include the long-range correlation energy. The exact energy is formally the sum of the RSH energy and the long-range correlation energy:

$$E_{\text{exact}} = E_{\text{RSH}} + E_c^{lr} \tag{7}$$

as depicted schematically in Fig. 1. Whereas for instance dispersion interactions are often added to DFT via *ad hoc* corrections based on the evaluation of atomic polarizabilities [17–19], the RS-DFT formalism allows us to include explicitly these important contributions to intermolecular interactions, only based on (i) the single parameter of the range separation μ, (ii) the choice of the short-range exchange-correlation functional, and (iii) the long-range correlation method. The long-range correlation energy can be calculated by second-order Møller–Plesset (MP2) perturbation theory [1], which leads to exactly the same equations as standard MP2 [20], i.e., for closed-shell systems:

$$E_{c,MP2}^{lr} = \sum_{ijab} \frac{[2(ia|jb)^{lr} - (ib|ja)^{lr}](ia|jb)^{lr}}{\epsilon_i + \epsilon_j - \epsilon_a - \epsilon_b}, \tag{8}$$

where i, j and a, b refer to occupied and virtual RSH orbitals, respectively, and $(ia|jb)^{lr}$ are the long-range two-electron integrals (using the "erf" interaction). Of course, all these quantities (integrals and orbital energies) depend on the range-separation parameter μ. Similarly, the long-range correlation energy can be calculated by coupled-cluster singles, doubles and perturbative triples (CCSD(T)) [3, 21].

One of the central advantages of these methods with respect to standard quantum chemistry approaches like MP2 or coupled-cluster theory is the considerably weaker basis-set dependence as the short-range correlation hole is taken already into account via the density-functional part. As a consequence, basis-set superposition errors (BSSE) should be significantly reduced with respect to standard wave-function-based correlation calculations.

Concerning the short-range exchange-correlation functional, several approximations [16, 21–27] have been proposed. We employed from the different possibilities the short-range local-density approximation (LDA) of Ref. [25] and the short-range Perdew–Burke–Ernzerhof (PBE)

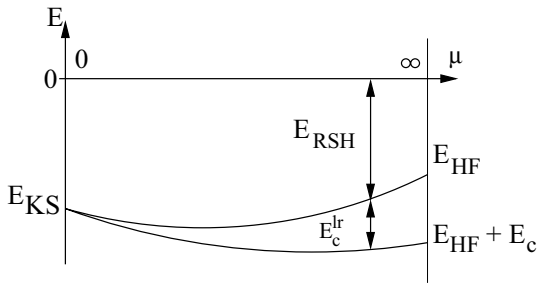

Fig. 1 Schematical composition of the RS-DFT total energy as the RSH energy plus the long-range correlation energy. For $\mu = 0$, one obtains standard Kohn–Sham theory without explicit long-range correlation correction, and for $\mu \to \infty$ RSH reduces to HF (no short-range functional) to which the correlation energy is added

functional of Ref. [22]. We will refer to the range-separated methods as RSHLDA + MP2 and RSHLDA +CCSD(T), and RSHPBE + MP2 and RSHPBE + CCSD(T). Of course, setting the range-separation parameter μ to infinity, we obtain the standard MP2 or CCSD(T) approach without a density-functional part.

3 Brief review of existing data

In the past, Be clusters have been abundantly studied, and an outstanding object of interest is the dimer (for a recent review, see [28]). Compared to the heavier alkaline-earth dimers, Be_2 already shows a shorter and stronger binding than expected for a purely dispersive interaction with an interatomic equilibrium distance and cohesion energy of about 2.4 Å and 2.5 kcal/mol, respectively.

This binding energy and interatomic distance have been a subject of long debates, experimentally and theoretically (see Refs. [6–12]). The experimental difficulties are summarized in a recent article [13], and from the theoretical side both the near degeneracy of the occupied 2*s* orbital with the unoccupied 2*p* orbitals [29, 30] and the shallowness of the potential well without being a purely dispersion interaction require a careful treatment of electron correlation [28].

It is therefore not surprising that at the HF level, Be_2 is not bound at all. Single-reference configuration-interaction (CI) schemes truncated at the level of single and double excitations (CISD) are not suited for this system [29, 31], even when including all exclusion-principle-violating (EPV) diagrams in a coupled-electron-pair approximation (called full CEPA or self-consistent size-consistent CI) [32]. One has to go indeed to multi-reference or coupled-cluster (including triple excitations [31, 33]) correlation methods for a correct description.

With the work of Røeggen and Veseth [9], Patkowski et al. [12], Schmidt et al. [11], and corresponding experimental data [13], we can consider that the potential well of the Be dimer is precisely known. DFT with usual semilocal approximations overestimates the interaction energy; however, the work of Jones [6] was the first theoretical one to claim the Be dimer to be significantly bound. RS-DFT with long-range MP2 or random-phase-approximation (RPA) approaches was applied to the Be dimer [2, 34, 35], giving significantly underestimated interaction energies. Range separation in combination with multi-reference perturbation theory (NEVPT2) has been published by Fromager et al. [36] with the conclusion that differences to the reference data despite the multi-reference long-range correlation treatment should be imputed to deficiencies of the employed short-range PBE functional.

For Be_3 in D_{3h} symmetry, HF theory gives no overall binding [37–41]. Nevertheless, a distinct local minimum is produced, contrary to Be_2 where the HF potential curve is purely repulsive. Including electron correlation [37–41] results in a cohesion energy of the triatomic "molecule" between 15 and 30 kcal/mol, with an equilibrium interatomic distance of about 2.2 Å, which is about the same as for the local minimum in HF. The significant difference in the binding of the dimer and the trimer (i.e., the importance of non-additivity or "3-body interactions") has been discussed by Novaro and Kołos [42] and Daudey et al. [43] already in the 1970s in the framework of HF theory. A comparative study [44] of the dimer, trimer and tetramer of Be and of Mg, based on MP2, CCSD(T), and DFT methods, estimates the utility of different basis-set extrapolation formulae and concludes that an extrapolation from the difference between double-zeta and triple-zeta basis sets is sufficient to estimate converged results for binding energies. As in the case of rare-gas dimers and the Be dimer, the LDA overestimates the binding energy of the trimer [45, 46]. Even gradient-corrected functionals such as BPW91 result in too high binding energies [47], the effect being less important but still present for the B3LYP hybrid functional [48].

4 Results and discussion

In order to dispose of a coherent reference dataset for the two systems, we perform MP2, MP4, CCSD(T), MRCI, MR-ACPF [49], and MR-AQCC [50–52] calculations with the MOLPRO program package [53]. For the multi-reference calculations, two electrons and four orbitals of each Be atom are included in the complete active space (CAS), forming the reference space to which single and double excitations in the size-consistency-corrected ACPF or AQCC correlation formalism are added.

We employ the aug-cc-pV*X*Z basis sets (X = D, T, Q — see "Appendix"), and for the reference calculations we extrapolate the correlation energy via the inverse-cubic scheme $E_c(X) = E_c(\infty) + B/X^3$ to an estimate of the complete (valence) basis-set limit. For RS-DFT calculations, however, it has been shown that an exponential form $E_c(X) = E_c(\infty) + B\exp(-\beta X)$ is more adequate [54]—we will therefore employ this scheme for the RS-DFT results. All data are corrected for the BSSE by the counterpoise scheme of Boys and Bernardi [55], even though this correction remains always smaller than 0.2 kcal/mol. The HF energy is considered to be converged with the quadruple-zeta basis set.

For the wave-function-based correlation calculations, the core orbitals were kept frozen, i.e., only the valence shells are explicitly correlated. Indeed, this choice is consistent with the fact that the aug-cc-pV*X*Z basis sets do not contain functions to correlate core electrons. In the short-range functional, however, core correlation is automatically included

even when long-range correlation is treated by a frozen-core wave-function-based method.

In order to study core-valence correlation explicitly, we did some exploratory calculations with the core-polarization potentials (CPPs) of the Stuttgart group [56] added to the frozen-core calculations, as well as correlated all-electron calculations in an aug-cc-pwCVTZ basis set with core functions [57] added to the standard aug-cc-pVTZ set.

4.1 Wave-function-based reference calculations

For the dimer, the extrapolated MR-ACPF and MR-AQCC interaction energy curves are close to the reference potential of Refs. [9] or [12] (see Table 1, left column for bond lengths and potential depths), while the CCSD(T) curve has a similar shape but underestimates the interaction energy significantly (see Supplementary material for data and graph). As discussed above, CCSD is not at all adequate here, and perturbation theory yields as well quite different interaction potentials, MP2 underestimating at the equilibrium distance and MP4 overestimating at larger distances.

For the trimer (see Fig. 2), we do not dispose of an accurate reference curve from the literature, but we see that CCSD(T) and multi-reference methods give potentials of similar shape, and again second-order perturbation theory yields significantly different results, but in the opposite way with respect to Be_2. MP4 overestimates the interaction energy as much as CCSD(T) underestimates it (Table 1, right column). CCSD again largely underbinds.

By taking into account core and core-valence correlations, the interaction energy is lowered (in a triple-zeta basis set) by about 0.1 kcal/mol for the all-electron calculations, and by about 0.4 kcal/mol using the CPPs, for the dimer. For the Be trimer, the effect is about 1 kcal/mol for the inclusion of core correlations and about 4 kcal/mol for the use of the CPPs. We thus use the frozen-core data, and, due to these estimations, we keep in mind that the true interaction potential may be slightly lower than our actual multi-reference data.

Table 1 Equilibrium bond lengths (Å) and interaction energies (kcal/mol) from inverse-cubic basis-set extrapolated potential curves for the Be dimer and trimer

	Be_2		Be_3	
	$r_{Be\text{-}Be}$	E_{min}	$r_{Be\text{-}Be}$	E_{min}
MP2	2.71	− 1.32	2.20	− 30.7
MP4	2.52	− 2.38	2.22	− 28.8
CCSD	4.42	− 0.17	2.21	− 14.4
CCSD(T)	2.48	− 1.87	2.21	− 24.0
MRCI	2.47	− 2.40	2.20	− 25.9
MR-ACPF	2.46	− 2.52	2.20	− 26.7
MR-AQCC	2.46	− 2.44	2.20	− 26.4

See text for the extrapolation procedure

4.2 RS-DFT calculations

From the previous section, we conclude that today's "gold standard" CCSD(T) with basis-set extrapolation gives for the trimer too low a cohesion energy, by about 2.5 kcal/mol or 10%. The calculations need a non-negligible effort, which may be avoided by resorting to DFT-based calculations while resulting in not worse an error. In Fig. 3, we display

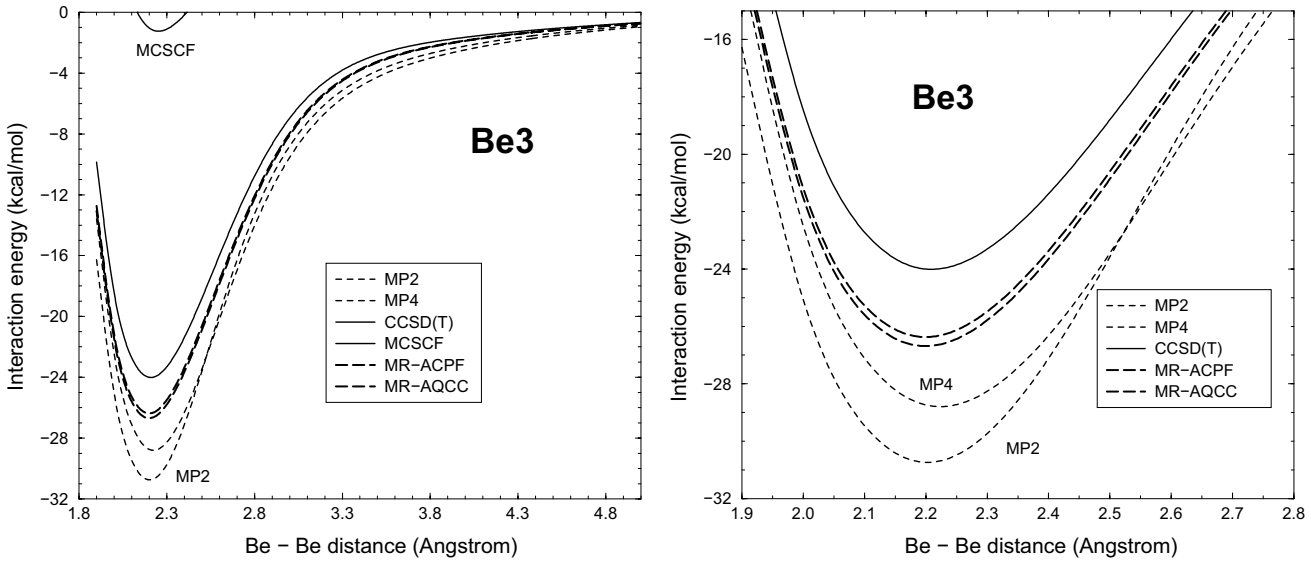

Fig. 2 Basis-set extrapolated interaction energy curves for the Be trimer, as obtained by wave-function-based methods. The right panel is a zoom into the minimum-energy region of the left panel

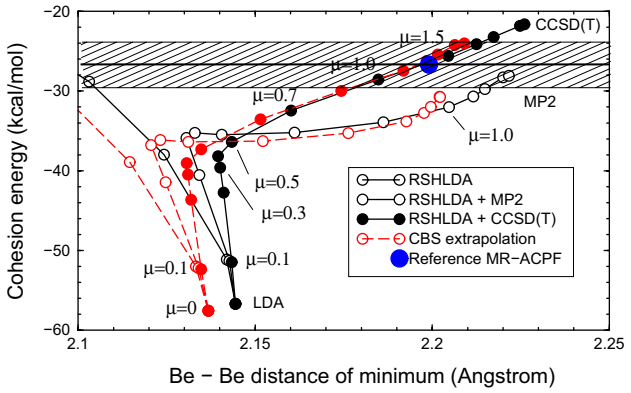

Fig. 3 Effect of the basis-set extrapolation for the equilibrium cohesion energies and bond lengths as a function of the range-separation parameter μ, for Be_3. Full lines are for the aug-cc-pVTZ basis set, and dashed lines represent the corresponding extrapolated values

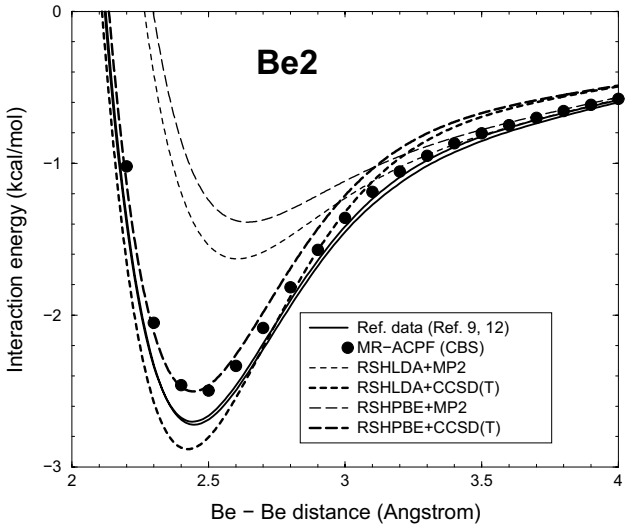

Fig. 4 Interaction energy curves of the RS-DFT methods for the Be dimer, compared to the reference data. Basis set is the aug-cc-pVTZ one, and the range-separation parameter μ is taken equal to 1 a.u.. Of the corresponding curves, the RSHPBE ones lie always above the RSHLDA ones

the evolution of the RS-DFT interaction energies with the range-separation parameter μ, in comparison with our MR-ACPF reference data, and the "region of confidence" around the reference energy as shaded area, which we chose to be the deviation of basis-set extrapolated CCSD(T) around the MR-ACPF reference. In order to remain inside this region, we may take a value for the range-separation parameter μ between 0.7 and 1.7 a.u., and either short-range functional combined with long-range CCSD(T). In the figure, we see as well the reduction in the influence of the extrapolation procedure when going from large μ to $\mu = 0$.

For simplicity, we will use for further comparisons $\mu = 1.0$ a.u. at the lower end of the interval of confidence, however significantly larger than the commonly employed value of 0.5 a.u. (see, e.g., Refs. [5, 22, 58]). For this value of $\mu = 1.0$ a.u., the contribution from the short-range functional with its advantages (low computational cost, small basis-set superposition error, and weak basis-set dependence) is still present. Without loosing too much in accuracy, we still may carry out the calculations in the aug-cc-pVTZ basis set.

Figures 4 and 5 show the RSHLDA + MP2, RSHPBE + MP2, RSHLDA + CCSD(T) and RSHPBE + CCSD(T) interaction energies with aug-cc-pVTZ basis for $\mu = 1$ a.u., for the dimer and for the trimer, in comparison with the available reference data. The equilibrium bond lengths and interaction energies obtained from RS-DFT calculations with a series of basis sets are reported in Table 2, and compared to those obtained from standard DFT, MP2, and CCSD(T) calculations.

Calculations with standard density-functional approximations overestimate the interaction energies considerably. For instance in the case of the dimer with a factor of 5 for LDA, and still a factor of 1.5 for B3LYP. RSHLDA + CCSD(T) and RSHPBE + CCSD(T) produce interaction energies in good agreement with the reference data. In contrast, RSHLDA + MP2 and RSHPBE + MP2 significantly underbind the dimer and overbind the trimer, as we have seen already from Figs. 4 and 5. Note that for Be_3, RSH + CCSD(T) (Fig. 5) and CCSD(T) (Fig. 2) give the same deviation from the reference data for large interatomic distances.

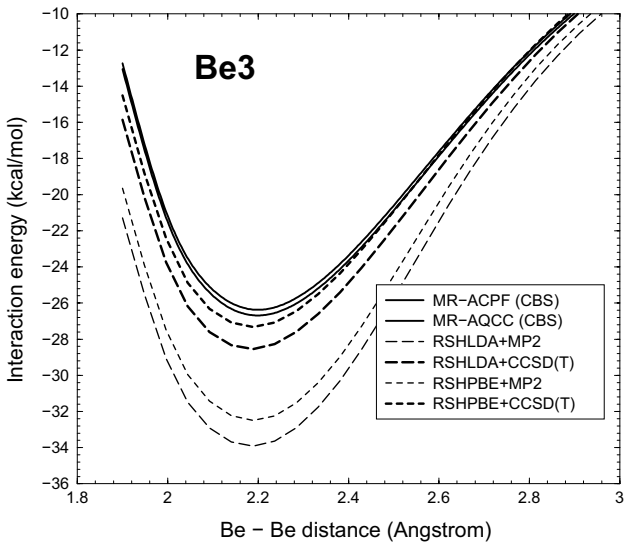

Fig. 5 Interaction energy curves of the RS-DFT methods for the Be trimer, compared to our own reference data. Same parameters as for Fig. 4. RSHLDA interaction energies are always smaller than the RSHPBE ones

Table 2 Equilibrium bond lengths (Å) and interaction energies (kcal/mol) for different methods and basis sets for the Be dimer and trimer

	aug-cc-pVDZ		aug-cc-pVTZ		aug-cc-pVQZ	
	$r_{\text{Be-Be}}$	E_{min}	$r_{\text{Be-Be}}$	E_{min}	$r_{\text{Be-Be}}$	E_{min}
Be_2						
LDA	2.44	− 12.5	2.46	− 12.8	2.33	− 12.9
PBE	2.45	− 9.5	2.44	− 9.7	2.43	− 9.8
B3LYP	2.51	− 3.9	2.49	− 4.1	2.40	− 4.1
MP2	–	–	2.83	− 0.9	2.74	− 1.2
CCSD(T)	–	–	2.54	− 1.2	2.50	− 1.6
RSHLDA $\mu = 1$	–	–	–	–	–	–
RSHPBE $\mu = 1$	–	–	–	–	–	–
RSHLDA + MP2 $\mu = 1$	2.65	− 1.0	2.61	− 1.6	2.59	− 1.8
RSHPBE + MP2 $\mu = 1$	2.69	− 0.8	2.64	− 1.4	2.63	− 1.5
RSHLDA + CCSD(T) $\mu = 1$	2.45	− 2.0	2.42	− 2.9	2.41	− 3.1
RSHPBE + CCSD(T) $\mu = 1$	2.48	− 1.6	2.44	− 2.5	2.44	− 2.7
Be_3						
LDA	2.17	− 54.7	2.14	− 56.7	2.14	− 57.2
PBE	2.20	− 44.8	2.18	− 46.2	2.17	− 46.6
B3LYP	2.18	− 29.6	2.16	− 31.2	2.16	− 31.5
MP2	2.26	− 23.0	2.22	− 28.1	2.21	− 29.7
CCSD(T)	2.27	− 16.2	2.23	− 21.6	2.22	− 23.1
RSHLDA $\mu = 1$	2.15	− 9.2	2.11	− 10.8	2.11	− 11.2
RSHPBE $\mu = 1$	2.15	− 7.7	2.12	− 9.0	2.12	− 9.4
RSHLDA + MP2 $\mu = 1$	2.21	− 30.6	2.19	− 33.9	2.18	− 34.7
RSHPBE + MP2 $\mu = 1$	2.21	− 29.3	2.19	− 32.5	2.18	− 33.2
RSHLDA + CCSD(T) $\mu = 1$	2.21	− 24.9	2.18	− 28.5	2.18	− 29.3
RSHPBE + CCSD(T) $\mu = 1$	2.21	− 23.8	2.19	− 27.3	2.18	− 28.0

For the Be_2 case, the energy differences due to different basis sets are small, and we may look first at the Be_3 results. We see that if we take the difference in binding energies between the DZ and TZ as one, the difference between TZ and QZ is about one quarter, consistently for all methods. In absolute values, the differences due to the basis sets are divided by a factor of two between MP2/CCSD(T) and the RS-DFT interaction energies. However, using RS-DFT this dependence is twice as large as for the pure density-functional calculations, employing the standard functionals LDA, PBE, B3LYP or the short-range functionals only. The same factor of 4 between the DZ–TZ and the TZ–QZ differences is found in the case of the Be_2 in the RS-DFT calculations.

Let us look in more detail into the RS-DFT calculations (Figs. 6, 7). Varying the range-separation parameter, we determine the minima of the cohesion-energy curves, which all lie in a narrow range of distances, but not on energies. Again, we note that MP2 and CCSD(T) long-range correlations have not the same effect on the results. Indeed, when aiming at reproducing the reference calculations, electron correlation of order higher than second-order perturbation theory is needed. This is more pronounced in Be_2 than in Be_3, where RSH + MP2 or RSH + CCSD(T) follow similar trends with the

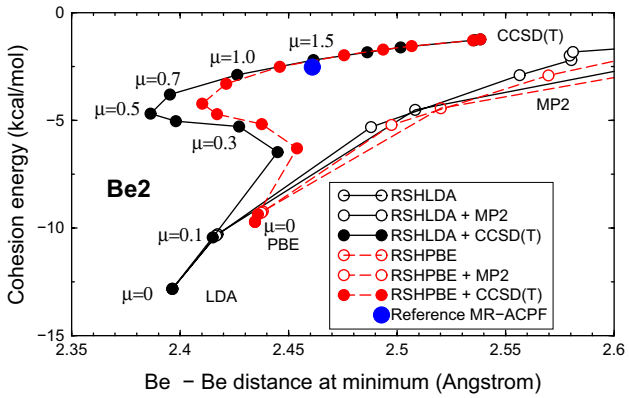

Fig. 6 Equilibrium cohesion energies and bond lengths as a function of the range-separation parameter μ, for Be_2 and the aug-cc-pVTZ basis set. We include our basis-set extrapolated MR-ACPF/AQCC reference point

range-separation parameter μ. The interpolation between $\mu = 0$ (pure Kohn–Sham DFT) and $\mu \to \infty$ (no contribution of a functional) appears to be not at all linear, neither for Be_2 nor for Be_3, and the optimal range-separation parameter should be chosen significantly larger than 0.5 a.u., as found before. Of course, for large μ the difference

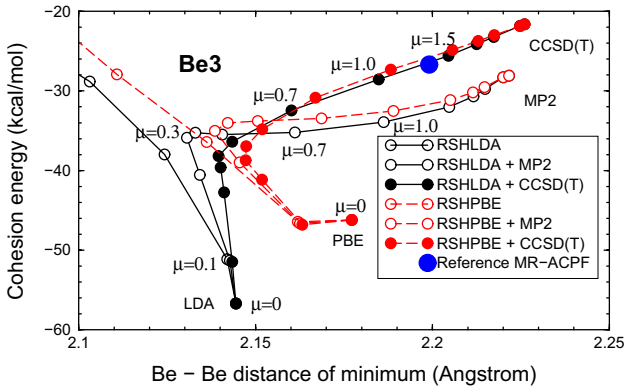

Fig. 7 Equilibrium cohesion energies and bond lengths as a function of the range-separation parameter μ, for Be_3 and the aug-cc-pVTZ basis set

between the two functionals employed becomes reasonably small.

Before concluding, we might look at the performances of other recent DFT approaches as provided by the double-hybrid functionals including both HF exchange and a MP2 correlation part. Thus, results should lie somewhere between standard MP2 and our RSH + MP2. Using the B2PLYP [59], the XYG3 [60], and the ωB97X-2(TQZ) [61] functionals, we find indeed (data in the Supplementary Material) for the trimer that all functionals overshoot as did MP2 and RSH + MP2 already. For the dimer, the situation is a little different as MP2 and RSH + MP2 resulted in a too weak interaction, but the double hybrids overbind, and the three variants lead to significantly different shapes of the potential.

5 Conclusion

We investigated the challenging systems Be_2 and Be_3 with different wave-function and DFT methods, comparing these to RS-DFT approaches, which are capable of describing explicitly long-range correlations, absent in standard Kohn–Sham theory with semilocal approximations. The interaction energy in small Be clusters is certainly not only due to dispersion as the interatomic distances are far smaller than typical van der Waals interactions, and interaction energies are much higher.

We observe that for this particular type of bonding—no chemical bond properly speaking, but no dispersion-only binding either (as for rare-gas complexes)—the RS-DFT approach, when used with the usual range-separation parameter of $\mu = 0.5$ a.u., produces too high binding energies, similar to the commonly employed B3LYP functional. Using a value of μ around 1 a.u. in our RS-DFT scheme with a CCSD(T) long-range part permits to reproduce well the MR–ACPF or MR–AQCC reference energies of the trimer.

Long-range single-reference CCSD(T) thus seems adequate for obtaining a reliable binding energy—even if perhaps due to fortuitous error cancelation. On the other hand, adding only second-order diagrams for expanding the long-range correlation energy is not sufficient, for any value of the range-separation parameter. This last point is in particular important for the modern development of double hybrids, leaving room for further developments.

Acknowledgements This work has been partly financed by the French ANR (Agence Nationale de la Recherche) through Contract Nr. ANR 07-BLAN-0272 (project Wademecom). The authors thank D. Andrae (Berlin), H. Stoll (Stuttgart) and F. Spiegelmann (Toulouse) for fruitful hints. Computer time has been provided by the Fédération de Recherche IP2CT (Sorbonne University, Paris).

Appendix: Technical details

All calculations were performed on 3.3 GHz Intel PCs running CentOS Linux, using Molpro [53] in its version 2008.2 (standard DFT and MCSCF/MRCI calculations) and a local development version, 2008.2, for the RS-DFT calculations. The employed aug-cc-pVXZ basis sets originate from the Gaussian basis set exchange form at Pacific National Laboratories. Only for the calculations on double hybrids, we employed the QChem code, version 5.0 [62].

For the single- and multi-reference methods and the long-range correlation part of the RS-DFT calculations, only the valence electrons of the Be atom were correlated. Energy thresholds were 10^{-7}a.u. for convergence and 10^{-9}a.u. as target accuracy for establishing the grid for the numerical density-functional integration.

The multi-reference calculations started from a complete-active-space (CAS) wave function with the two valence electrons in four orbitals for each atom. The subsequent ACPF or AQCC calculations used this CAS wave function as reference space (60 configuration state functions (CSFs) for Be_2, and about 4000 CSFs for Be_3).

Minima in the 1D potential curves were determined through a spline fit with points spaced at 0.1 Å, starting at 1.9 Å and including some large distances to check size consistency.

References

1. Ángyán JG, Gerber IC, Savin A, Toulouse J (2005) Phys Rev A 72:012510
2. Toulouse J, Zhu W, Angyan JG, Savin A (2010) Phys Rev A 82:032502
3. Toulouse J, Zhu W, Savin A, Jansen G, Àngyàn JG (2011) J Chem Phys 135:084119
4. Chermak E, Mussard B, Ángyán JG, Reinhardt P (2012) Chem Phys Lett 550:162

5. Mussard B, Reinhardt P, Àngyán JG, Toulouse J (2015) J Chem Phys 142:154123
6. Jones RO (1979) J Chem Phys 71:1300
7. Liu B, McLean AD (1980) J Chem Phys 72:3418
8. Bondybey VE (1984) Chem Phys Lett 109:436
9. Roggen I, Veseth L (2005) Int J Quant Chem 101:201
10. Patkowski K, Podeszwa R, Szalewicz K (2007) J Phys Chem A 111:12822
11. Schmidt MW, Ivanic J, Ruedenberg K (2010) J Phys Chem A 114:8687
12. Patkowski K, Spirko V, Szalewicz K (2009) Science 326:1382
13. Merritt JM, Bondybey VE, Heaven MC (2009) Science 324:1548
14. Kalemos A (2016) J Chem Phys 145:214302
15. Kohn W, Sham LJ (1965) Phys Rev 140:A1133
16. Toulouse J, Colonna F, Savin A (2004) Phys Rev A 70:062505
17. Grimme S (2004) J Comput Chem 25:1463
18. Elstner M, Hobza P, Frauenheim T, Suhai S, Kaxiras E (2001) J Chem Phys 114:5149
19. Becke AD, Johnson ER (2005) J Chem Phys 122:154104
20. Møller C, Plesset MS (1934) Phys Rev 46:618
21. Goll E, Werner HJ, Stoll H (2005) Phys Chem Chem Phys 7:3917
22. Goll E, Werner HJ, Stoll H, Leininger T, Gori-Giorgi P, Savin A (2006) Chem Phys 329:276
23. Toulouse J, Savin A, Flad HJ (2004) Int J Quant Chem 100:1047
24. Toulouse J, Colonna F, Savin A (2005) J Chem Phys 122:014110
25. Paziani S, Moroni S, Gori-Giorgi P, Bachelet GB (2006) Phys Rev B 73:155111
26. Fromager E, Toulouse J, Jensen HJAa (2007) J Chem Phys 126:074111
27. Goll E, Ernst M, Moegle-Hofacker F, Stoll H (2009) J Chem Phys 130:234112
28. Heaven MC, Merritt JM, Bondybey VE (2011) Ann Rev Phys Chem 62:375
29. Harrison RJ, Handy NC (1983) Chem Phys Lett 98:97
30. Lepetit MB, Malrieu JP (1990) Chem Phys Lett 169:285
31. Zhang H, Ma J, Reinhardt P, Malrieu JP (2009) J Chem Phys 132:034108
32. Daudey JP, Heully JL, Malrieu JP (1993) J Chem Phys 99:1240
33. Sosa C, Noga J, Bartlett RJ (1988) J Chem Phys 88:5974
34. Gerber IC, Ángyán JG (2005) Chem Phys Lett 416:370
35. Toulouse J, Gerber IC, Jansen G, Savin A, Àngyán JG (2009) Phys Rev Lett 102:096404
36. Fromager E, Chimiraglia R, Jensen HJAa (2010) Phys Rev A 81:024502
37. Harrison RJ, Handy NC (1986) Chem Phys Lett 123:321
38. Lee TJ, Rendell AP, Taylor PR (1990) J Chem Phys 92:489
39. Kaplan IG, Roszak S, Leszczynski J (2000) J Chem Phys 113:6245
40. Klopper W, Almlöf J (1993) J Chem Phys 99:5167
41. Junquera-Hernández JM, Sánchez-Marín J, Bendazzoli GL, Evangelisti S (2004) J Chem Phys 120:8405
42. Novaro O, Kołos W (1967) J Chem Phys 67:5066
43. Daudey JP, Novaro O, Kołos W, Berrondo M (1979) J Chem Phys 71:4297
44. Jae SL (2003) Phys Rev A 68:43201
45. Khanna SN, Reuse F, Buttet J (1988) Phys Rev Lett 61:535
46. Rao BK, Khanna SN, Meng J, Jena P (1991) Z Phys D 18:171
47. Sriniva S, Jellinek J (2004) J Chem Phys 121:7243
48. Beyer MK, Kaledin LA, Kaledin AL, Heaven MC, Bondybey VE (2000) Chem Phys 262:15
49. Gdanitz R, Ahlrichs R (1988) Chem Phys Lett 143:413
50. Meissner L (1988) Chem Phys Lett 146:205
51. Szalay PG, Bartlett RL (1993) Chem Phys Lett 214:481
52. Füsti-Molnár L, Szalay PG (1996) Chem Phys Lett 258:400
53. Molpro 2006.1 and 2008.2; MOLPRO is a package of ab-initio programs written by Werner HJ and Knowles PJ with contributions from Almlöf J, Amos RD, Bernhardsson A, Berning A, Cooper DL, Deegan MJO, Dobbyn AJ, Eckert F, Hampel C, Lindh R, Lloyd AW, Meyer W, Mura ME, Nicklass A, Peterson K, Pitzer R, Pulay P, Rauhut G, Schütz M, Stoll H, Stone AJ, Taylor PR, Thorsteinsson T, University of Stuttgart and Birmingham (1998)
54. Franck O, Mussard B, Luppi E, Toulouse J (2015) J Chem Phys 142:074107
55. Boys SF, Bernardi F (1970) Mol Phys 19:553
56. Stoll H, Fuentealba P, Schwerdtfeger P, Flad J, v. Szentpály L, Preuss HW (1984) J Chem Phys 81:2732
57. Peterson K (2009) Private communication
58. Gerber IC, Ángyán JG (2005) Chem Phys Lett 415:100
59. Grimme S (2009) J Chem Phys 124:034108
60. Zhang Y, Xu X, Goddard WA III (2009) Proc Natl Acad Sci USA 106:4963
61. Chai J-D, Head-Gordon M (2009) J Chem Phys 131:174105
62. Shao Y, Gan Z, Epifanovsky E, Gilbert ATB, Wormit M, Kussmann J, Lange AW, Behn A, Deng J, Feng X, Ghosh D, Goldey M, Horn PR, Jacobson LD, Kaliman I, Khaliullin RZ, Kús T, Landau A, Liu J, Proynov EI, Rhee YM, Richard RM, Rohrdanz MA, Steele RP, Sundstrom EJ, Woodcock HL III, Zimmerman PM, Zuev D, Albrecht B, Alguire E, Austin B, Beran GJO, Bernard YA, Berquist E, Brandhorst K, Bravaya KB, Brown ST, Casanova D, Chang CM, Chen Y, Chien SH, Closser KD, Crittenden DL, Diedenhofen M, DiStasio RA Jr, Dop H, Dutoi AD, Edgar RG, Fatehi S, Füsti-Molnar L, Ghysels A, Golubeva-Zadorozhnaya A, Gomes J, Hanson-Heine MWD, Harbach PHP, Hauser AW, Hohenstein EG, Holden ZC, Jagau TC, Ji H, Kaduk B, Khistyaev K, Kim J, King RA, Klunzinger P, Kosenkov D, Kowalczyk T, Krauter CM, Lao KU, Laurent A, Lawler KV, Levchenko SV, Lin CY, Liu F, Livshits E, Lochan RC, Luenser A, Manohar P, Manzer SF, Mao SP, Mardirossian N, Marenich AV, Maurer SA, Mayhall NJ, Oana CM, Olivares-Amaya R, OâĂŹ Neill DP, Parkhill JA, Perrine TM, Peverati R, Pieniazek PA, Prociuk A, Rehn DR, Rosta E, Russ NJ, Sergueev N, Sharada SM, Sharmaa S, Small DW, Sodt A, Stein T, Stück D, Su YC, Thom AJW, Tsuchimochi T, Vogt L, Vydrov O, Wang T, Watson MA, Wenzel J, White A, Williams CF, Vanovschi V, Yeganeh S, Yost SR, You ZQ, Zhang IY, Zhang X, Zhou Y, Brooks BR, Chan GKL, Chipman DM, Cramer CJ, Goddard WA III, Gordon MS, Hehre WJ, Klamt A, Schaefer HF III, Schmidt MW, Sherrill CD, Truhlar DG, Warshel A, Xua X, Aspuru-Guzik A, Baer R, Bell AT, Besley NA, Chai JD, Dreuw A, Dunietz BD, Furlani TR, Gwaltney SR, Hsu CP, Jung Y, Kong J, Lambrecht DS, Liang W, Ochsenfeld C, Rassolov VA, Slipchenko LV, Subotnik JE, Van Voorhis T, Herbert JM, Krylov AI, Gill PMW, Head-Gordon M (2015) Mol Phys 113:184